

In Vivo Validation of Patient-Specific Pressure Gradient Calculations for Iliac Artery Stenosis Severity Assessment

Stefan G. H. Heinen, PDEng; Daniel A.F. van den Heuvel, MD; Wouter Huberts, PhD; Sanne W. de Boer, MD; Frans N. van de Vosse, PhD; Tammo Delhaas, MD, PhD; Jean-Paul P. M. de Vries, MD, PhD

Background—Currently, the decision to treat iliac artery stenoses is mainly based on visual inspection of digital subtraction angiographies. Intra-arterial pressure measurements can provide clinicians with accurate hemodynamic information. However, pressure measurements are rarely performed because of their invasiveness and the time required. Therefore, the aim of the study was to test the feasibility of a computational model that can predict translesional pressure gradients across iliac artery stenoses on the basis of imaging data only.

Methods and Results—Patients (N=21) with symptomatic peripheral arterial disease and a peak systolic velocity ratio between 2.5 and 5.0 were included in the study. Patients underwent per-procedural 3-dimensional rotational angiography and hyperemic intra-arterial translesional pressure measurements. Vascular anatomical features were reconstructed from the 3-dimensional rotational angiography data into an axisymmetrical 2-dimensional computational mesh, and flow was estimated on the basis of the stenosis geometry. Computational fluid dynamics were performed to predict the pressure gradient and were compared with the measured pressure gradients. A good agreement by overlapping error bars of the predicted and measured pressure gradients was found in 21 of 25 lesions. Stratification of the stenosis on the basis of the predicted pressure gradient into hemodynamic not significant (<10 mm Hg) and hemodynamic significant (\geq 10 mm Hg) resulted in sensitivity, specificity, and overall predictive values of 95%, 60%, and 88%, respectively.

Conclusions—The feasibility of the patient-specific computational model to predict the hyperemic translesional pressure gradient over iliac artery stenosis was successfully tested. Presented results suggest that, with further optimization and corroboration, the model can become a valuable aid to the diagnosis of equivocal iliac artery stenosis.

Clinical Trial Registration—URL: <http://www.trialregister.nl>. Unique identifier: NTR5085. (*J Am Heart Assoc.* 2017;6:e007328. DOI: 10.1161/JAHA.117.007328.)

Key Words: angiography • blood pressure measurement/monitoring • diagnostic method • peripheral artery disease • stenosis

Intermittent claudication, a symptom of peripheral arterial disease (PAD), is characterized by exercise-induced severe muscle pain that is relieved after a short period of rest.¹ The pain results from insufficient blood supply to the extremities, caused by occlusive or stenotic lesions in the feeding arteries. However, it can be challenging to select stenoses that are hemodynamically significant and warrant treatment. This holds, in particular, for iliac artery stenoses with lumen reduction of \approx 50% because these so-called equivocal stenoses cause

clinical symptoms in some patients, but no symptoms in others.^{2,3} The main clinical challenge is, therefore, to determine which equivocal stenoses are hemodynamically significant, particularly in case of multiple stenoses.

Because of its superior spatial resolution, digital subtraction angiography is still considered the gold standard for stenosis severity assessment and treatment planning in PAD.^{4,5} Visual inspection of these images by the interventionalist is the fastest and easiest way to determine the

From the Departments of Vascular Surgery (S.G.H.H., J.-P.P.M.d.V.) and Radiology (D.v.d.H., S.W.d.B.), St Antonius Hospital, Nieuwegein, The Netherlands; Department of Biomedical Engineering, CARIM School for Cardiovascular Diseases, Maastricht University Medical Center, Maastricht, The Netherlands (S.G.H.H., W.H., T.D.); and Department of Biomedical Engineering, Eindhoven University of Technology, Eindhoven, The Netherlands (F.N.v.d.V.).

Accompanying Data S1, S2 and Figure S1 are available at <http://jaha.ahajournals.org/content/6/12/e007328/DC1/embed/inline-supplementary-material-1.pdf>

Correspondence to: Stefan G. H. Heinen, PDEng, Department of Vascular Surgery, St Antonius Hospital, Koekoekslaan 1, 3435 CM, Postbus 2500 Nieuwegein, The Netherlands. E-mail: s.heinen@antoniusziekenhuis.nl

Received August 4, 2017; accepted October 19, 2017.

© 2017 The Authors. Published on behalf of the American Heart Association, Inc., by Wiley. This is an open access article under the terms of the Creative Commons Attribution-NonCommercial License, which permits use, distribution and reproduction in any medium, provided the original work is properly cited and is not used for commercial purposes.

Clinical Perspective

What Is New?

- This study is the first to demonstrate that hemodynamic significance of iliac artery stenoses can be determined using a patient-specific model that predicts the pressure gradient on the basis of imaging information only.

What Are the Clinical Implications?

- The model-predicted assessed pressure gradient across iliac artery stenoses can replace the expensive, time-consuming, and cumbersome task of performing intra-arterial pressure gradient measurements.

degree of the stenosis but tends to underestimate stenoses with a lumen diameter reduction of 50% or less and to overestimate stenoses with >50% diameter reduction.^{6,7} In addition, visual assessment neglects hemodynamic factors, such as the local pressure gradient and flow, whereas these factors are the major determinants for sufficient blood supply to the peripheral tissue.

Although severity assessment and treatment of equivocal stenosis are better diagnosed using invasive pressure measurements,⁸ these measurements are not often performed, even though they result in more cost-effective^{9,10} and favorable symptomatic outcomes⁸ and are recommended by the guidelines.⁵ As a consequence, a significant number of patients with PAD undergo an unnecessary percutaneous transluminal angioplasty procedure with or without stent placement. Conversely, stenoses with ≈50% diameter reduction or multiple serial stenoses with a diameter reduction of <50% can be hemodynamic significant and might remain unrecognized, hereby remaining an important source for the complaints of the patient. A tool that provides the interventionalist with an accurate patient-specific pressure gradient, without the need to perform invasive intra-arterial pressure measurements, could be a valuable contribution to the diagnosis and treatment planning of PAD.

A computational model could replace the intra-arterial pressure measurements and aid diagnosis, just as it has shown potential for assessment of coronary stenoses.^{11–13} The aim of this study was to test the feasibility of a modeling approach (ie, to assess its capability to patient specifically predict the translesional pressure gradient) under hyperemic conditions across equivocal iliac artery stenosis.

Methods

The data, analytic methods, and study materials will not be made available to other researchers for purposes of reproducing the results or replicating the procedure. The Medical

Research Ethics Committee does not grant permission to share the data with others. In addition, the in-house developed finite-element solver (TFEM), which is required to reproduce the simulation results, cannot be made publicly available.

Study Design

This was a prospective, single-center, observational study. The study protocol was approved by the Medical Research Ethics Committees United, and all participants gave written informed consent.

Study Population

Patients at least 18 years old, with symptomatic PAD and single or multiple lesions of the common or external iliac artery, and with a peak systolic velocity ratio between 2.5 and 5.0 or a visual lumen reduction between 50% and 75% (assessed by preprocedural duplex ultrasonography) were asked to participate in this study. Patients with iliac occlusions, aneurysmatic disease, or dissections were excluded. Other exclusion criteria were renal insufficiency (estimated glomerular filtration rate, <30 mL/min per 1.73 m²), acute ischemia, or iodine-based contrast media allergy.

Procedure Protocol

After introduction of a 6F sheath into the common femoral artery, 5000 U of heparin was administered. Next, 3-dimensional (3D) rotational angiography (3DRA) was performed, which replaced the 2 standard orthogonal 2-dimensional digital subtraction angiography projections. The location of the equivocal stenosis was determined by the interventionalist on the basis of visual inspection of the 3DRA. Subsequently, a fluid-filled catheter (FFC; 4F/65 cm/0.038; Cobra, Cordis, Switzerland) was inserted and zeroed to the atmospheric pressure. A pressure-monitoring guidewire (ComboWire 9515; Volcano Inc, San Diego, CA) was inserted through and placed at the tip of the FFC, for calibration. Because the temperature dependence of the pressure-monitoring guidewire could affect measurements, the calibration was performed after a pause of 2 minutes to prevent a temperature-induced drift. The pressure-monitoring guidewire and FFC were then advanced proximal and distal from the stenosis, respectively, at locations that were considered healthy vessel parts. Pressures were measured at these locations under hyperemic conditions, induced by administering 500 μg nitroglycerin through the FFC. Pressure signals were digitally stored on the ComboMap (Volcano Inc). For diagnosis, the pressure gradient was obtained in real time

from the display of the ComboMap. Lesions were treated when the hyperemic time-averaged pressure gradient was >10 mm Hg.⁸

For accurate comparison of the measured pressure gradient with the predicted pressure gradient and because peak hyperemia only lasts for a short period, the absolute time-averaged pressure gradient over the stenosis was also calculated off-line. The time-dependent pressure gradient was calculated by subtracting the distal pressure from the proximal pressure signal. Subsequently, the time-averaged pressure was calculated for every heartbeat. The peak hyperemic pressure gradient and associated SD were calculated by averaging 5 consecutive heart cycles at maximal hyperemia. These interarterial pressure measurements were used for validation of the calculated pressure gradients predicted by the model.

Model-Based Translesional Pressure Gradient Calculation

To assess patient-specific translesional pressure gradients under hyperemic conditions by computational modeling, 3

consecutive steps were performed: (1) geometry reconstruction, (2) application of boundary conditions, and (3) calculation of the translesional pressure gradient.

In the first step, the stenosis geometry is extracted from the 3DRA images (Figure 1A and 1B). Most stenoses have a complex geometry consisting of multiple diffuse constrictions, resulting in a complex lesion with spatially varying diameters (Figure 1C). These pathological vessel segments are evaluated in this study. Using XpertCT (Philips Healthcare, Best, The Netherlands), a 3D volume with a voxel size of $0.47 \times 0.47 \times 0.47$ mm³ was reconstructed from 121 projections of the patient's vasculature and stored as digital imaging and communications in medicine data. The digital imaging and communications in medicine data were imported in noncommercially available software package (Vessel Explorer; Philips Healthcare) to segment the pathological vessel segment. Subsequently, its 3D information was transformed to center-line coordinates with corresponding local radius by assuming circular cross-sectional areas, resulting in 2-dimensional axisymmetrical meshes.

In the second step, patient-specific boundary conditions are defined at the inlet, outlet, and wall of the segmented

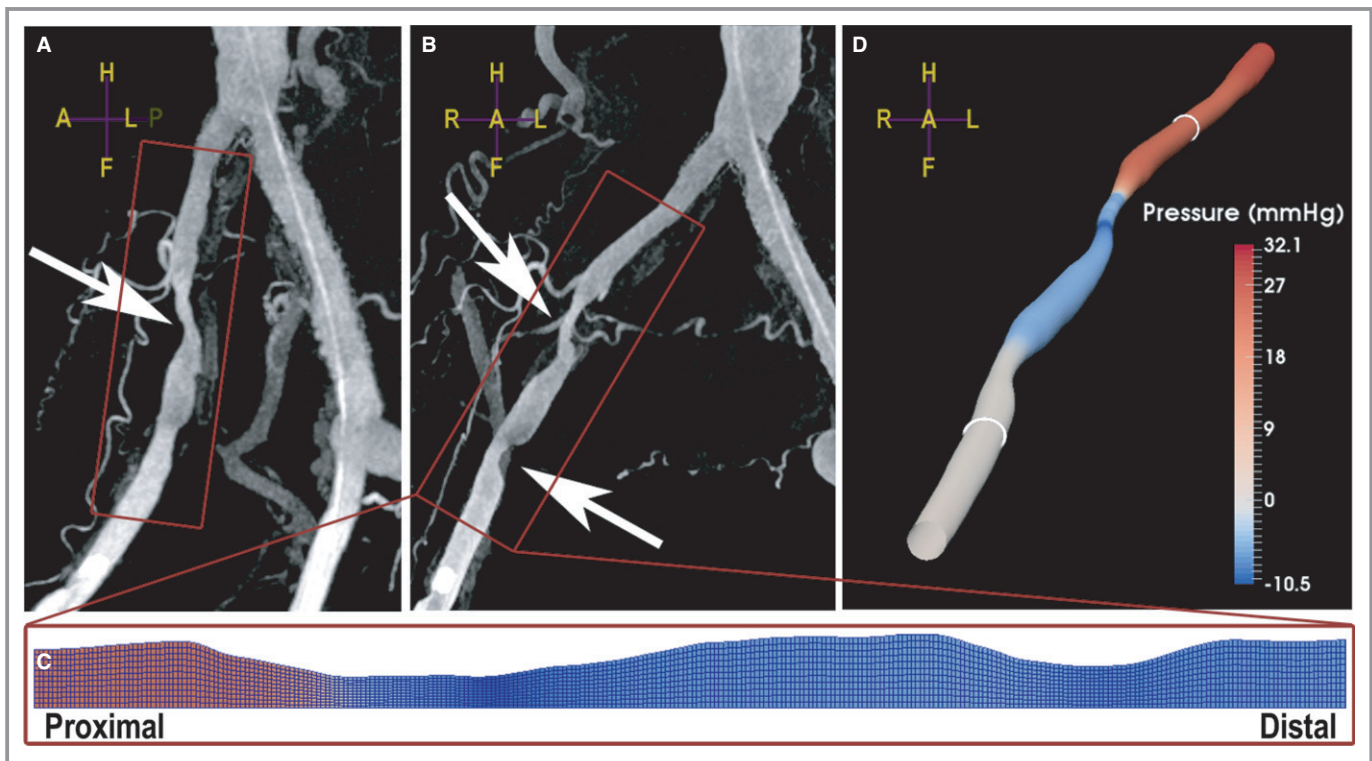


Figure 1. Example of predicted hyperemic pressure gradient estimated across an external iliac artery lesion (lesion 6) in a 62-year-old man. A and B, Representative 2 orthogonal angiographic projections from the 3-dimensional rotational angiogram, being left-right (A) and anterior-posterior (B). The arrows indicate the locations of the visually identified stenoses. C, The 2-dimensional mesh of the artery under study. D, The solution of the CFD problem is shown. The hyperemic predicted translesional pressure gradient was calculated between the white rings and found to be 26.8 ± 5.0 mm Hg. The in vivo measured hyperemic translesional pressure gradient was 24.5 ± 1.7 mm Hg; hence, the stenosis was considered hemodynamic significant and treated with an 8×80 -mm² self-expandable stent.

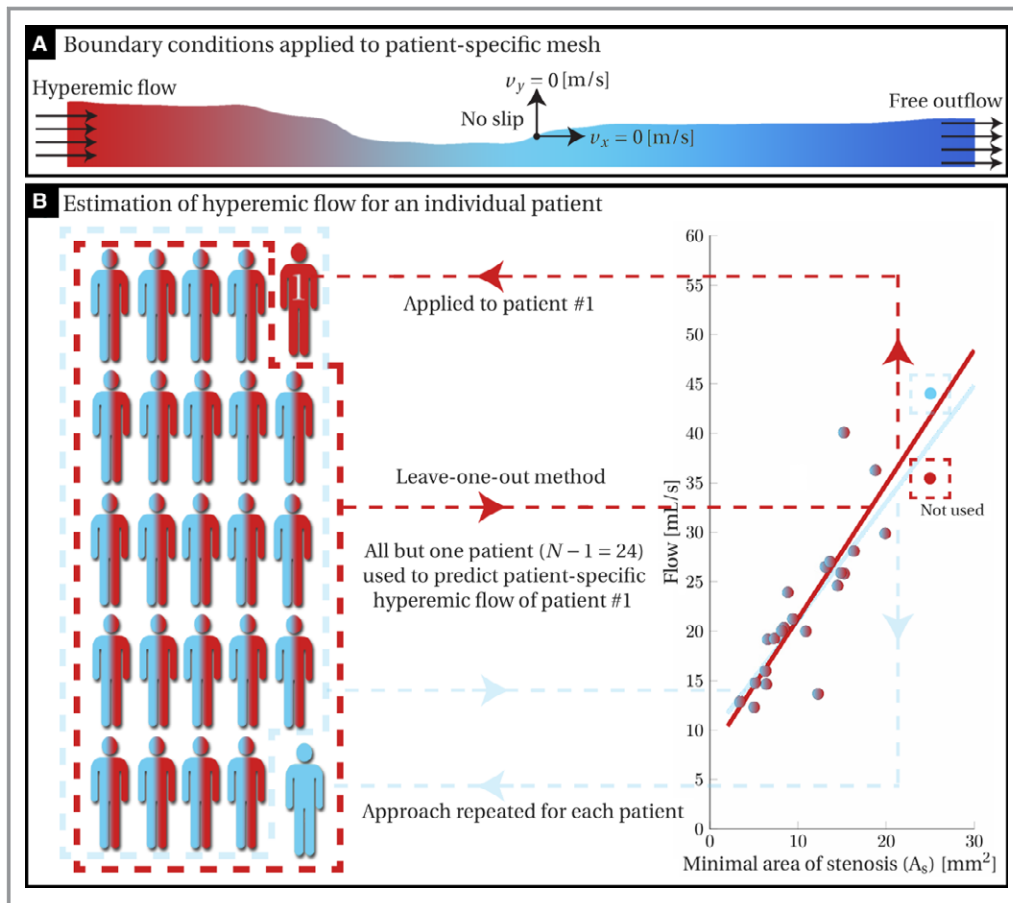


Figure 2. A schematic representation of the mesh and performed leave-one-out method, which was assessed to calculate the patient-specific hyperemic flow. A, The boundary conditions applied to a patient-specific mesh. B, Schematically outlines the leave-one-out method. The hyperemic flow relation of the patient depicted in red was estimated using the data points of all patients but one ($N - 1$), as enclosed by the red frame. The red data point that belongs to the patient depicted in red was not used in fitting the unique hyperemic relation. Subsequently, the derived relation (red line) was used to estimate the hyperemic flow for the patient depicted in red. The leave-one-out approach was conducted for every included patient (eg, the patient depicted in blue). It can be shown that, with increasing the number of patients, this approach becomes more accurate and converts to the population-averaged correlation (Data S1).

lesion (Figure 2A). At the vessel wall, we assume that no blood can pass through the arterial wall (impermeability) and that blood at the wall is stationary (no-slip condition; ie, $\vec{v} = \vec{0}$ [m/s]). A free-outlet condition is described, which will not alter the absolute pressure gradient across the stenosis because the simulation is inflow driven. Unfortunately in the current workflow, no hyperemic flow measurement is available. Therefore, we based the patient-specific hyperemic flow on an empirical relation between the hyperemic flow and the neck of the stenosis (Figure 2B).^{14,15} Because there is no historical cohort available, we determined the empirical relation on patient data of all patients included, except for the one for whom we want to estimate the mean hyperemic flow. This was done by an inverse modeling approach, a widely applied engineering method to assess unknown variables by using a model and known measurements. Herein, the patient-

specific geometry was used and known hyperemic flow (plug velocity profile¹⁶) was applied at the inlet, which makes it possible to calculate a pressure gradient over the stenosis. The calculated pressure gradient was then compared with the true measured pressure gradient. When the calculated pressure gradient equals the measured pressure gradient, the prescribed flow is likely equal to the real flow. Subsequently, a linear regression was applied to the optimized hyperemic flow for all patients, except one (leave-one-out method; Figure 2B). Given the minimal area at the neck of the stenosis of the patient under study, the hyperemic flow was estimated on the basis of the empirical relation of the other ones and applied as the inlet condition. This procedure was applied to every patient in our cohort.

The third and final step is the actual calculation of the translesional pressure gradient. The pressure gradient over

the stenosis is assessed by applying the described boundary conditions and solving the Navier-Stokes equations for an incompressible newtonian fluid by using a finite element method. The model was implemented in the in-house developed finite element package TFEM (Eindhoven University of Technology, Eindhoven, The Netherlands).¹⁷ The computational domain (stenosis geometry) consisted of 4000 rectangular quadratic (Taylor Hood) elements. A mesh convergence check showed that the error on the output of interest (Δp) was sufficiently small ($\text{error} < 5 \times 10^{-1}\%$) to reach a stable and accurate solution. For time discretization, we applied the Euler implicit difference scheme with time steps of 2.5 ms. Simulations were stopped when a steady solution was reached in all nodal points ($|p^{t+1} - p^t| < 0.01$ mm Hg). The absolute pressure gradient over the stenosis was then calculated from the proximal and distal pressure field by averaging over the cross-sectional area at the sites where in vivo measurements were performed (Figure 1D).

Simulation Analysis

Accuracy of pressure gradient calculations

To determine the number of accurate patient-specific pressure gradient estimates, good agreement between the measured and calculated translesional pressure gradient was defined as an overlap of the error bars. The error bar represents the uncertainty on the calculated pressure gradient. The presented prediction uncertainty results from the uncertainty of the estimated hyperemic flow, as indicated by the red dashed lines in Figure 3. The error bar on the measured hyperemic pressure gradient is the SD of the 5 averaged consecutive heart cycles at peak hyperemia.

Furthermore, the correlation between measured and calculated translesional pressure gradient was assessed by determining the R^2 with respect to the line $y=x$. For identifying the absolute bias between the in vivo measured and calculated translesional pressure gradient, the mean absolute difference and associated SDs were calculated. The agreement between the predicted and measured translesional pressure gradient was illustrated by a Bland-Altman plot.

Pressure gradient–based severity assessment

Measured and calculated hyperemic pressure gradients were stratified into 2 groups to assess the diagnostic value. According to the current guidelines, lesions were hemodynamic nonsignificant if $\Delta p < 10$ mm Hg or hemodynamic significant when $\Delta p \geq 10$ mm Hg.⁵ The diagnostic accuracy of the computational model was assessed by calculating the sensitivity, the specificity, the positive and negative predictive values, and the overall diagnostic value with their associated 95% confidence intervals (CIs). The 95% CI was calculated

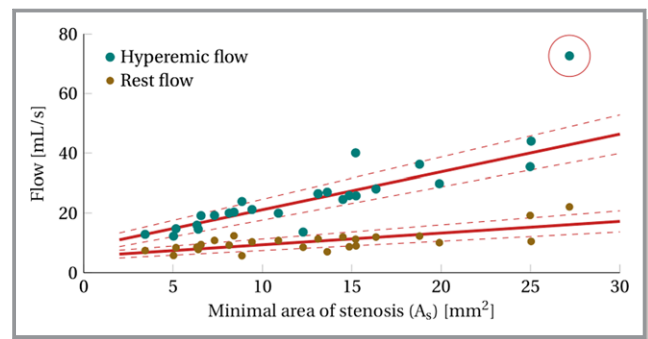


Figure 3. The retrospectively calculated mean hyperemic flow (green circles) using the patient-specific geometry and measured hyperemic pressure gradient. The correlation line fitted represents the population-averaged correlation using all study patients. The uncertainty (1 SD) of the correlation is indicated by the red dashed lines (Data S2). The circled patient is responsible for $>60\%$ of the residual sum of squares and, therefore, identified as an outlier (red circle). It can be shown that the same kind of relation holds for rest flow (yellow circles).

using the scoring method incorporating continuity correction.¹⁸

Results

Patient and Clinical Characteristics

Twenty-one patients (15 men) with a total of 25 lesions were recruited (Table 1). The median age was 67 years (range, 44–79 years). The median pain-free walking distance was 140 m (range, 40–320 m). Median rest ankle brachial index (ABI) was 0.73 (range 0.37–1.17), which decreased during exercise to a median of 0.46 (range 0.18–0.89). Fourteen lesions were located in the common iliac artery, and 11 lesions were located in the external iliac artery. Quantitative analysis of the 3DRA showed a median stenosis severity of 51% (range, 30%–78%) and a median lesion length of 24 mm (range, 12–63 mm). In addition, 9 patients had significant superficial femoral artery stenosis (N=6) or occlusions (N=3) besides the identified iliac artery stenosis. None of the patients had a popliteal artery stenosis.

Quantitative Accuracy of the Calculated Translesional Pressure Gradient

For every lesion, the in vivo measured and calculated pressure gradients during peak hyperemia are shown in Figure 4. A good agreement by overlapping error bars of the measured and calculated pressure gradient was found in 21 of the 25 lesions. Interestingly, all lesions with nonoverlapping error bars (lesions 5, 8, 15, and 18) correspond to the 4 points outside the 1 SD estimate of the hyperemic flow relation (Figure 3). The mean absolute difference and associated SD

Table 1. Baseline Characteristics of 21 Included Patients

Characteristics	Value
Age, y	67 (44–79)
Male sex	15 (71)
Cardiovascular risk factors	
Tobacco use	12 (57)
Diabetes mellitus	2 (10)
Hyperlipidemia	8 (38)
Hypertension	13 (62)
Clinical description	
ABI at rest	0.73 (0.37–1.17)
ABI after exercise	0.46 (0.18–0.89)
Pain-free walking distance, m	140 (40–320)
Comorbidities	
Stroke	4 (20)
Myocardial infarction	2 (10)
COPD	3 (15)
Medication	
Anticoagulants	21 (100)
Antihypertensive agents	13 (62)
Statins	13 (62)

Values are given as median (range) or number (percentage). ABI indicates ankle-brachial index; and COPD, chronic obstructive pulmonary disease.

between the in vivo and calculated translesional pressure gradient after administration of a vasodilator was -0.9 ± 12.7 mm Hg (mean \pm 2 SDs), which can be seen in the Bland-Altman plot shown in Figure 5. The R^2 between the calculated and in vivo measured hyperemic pressure gradient with respect to the line $y=x$ was 0.81 (Figure 6). It can be observed that the number of patients with a pressure gradient >40 mm Hg is limited. However, these lesions are of less interest because a large error on the pressure prediction will still likely indicate a hemodynamic significant stenosis ($\Delta p \geq 10$ mm Hg).

Severity Assessment of the Calculated Translesional Pressure Gradient

Lesions were assessed using our model and considered hemodynamically significant when the time-averaged pressure gradient was >10 mm Hg (Table 2), as indicated by the dashed black line in Figure 4. The model draws the same diagnostic conclusion in 22 of 25 lesions if compared with the intra-arterial measured pressure gradient, resulting in a sensitivity of 95% (95% CI, 76%–100%), a specificity of 60% (95% CI, 39%–78%), a positive predictive value of 90% (95% CI,

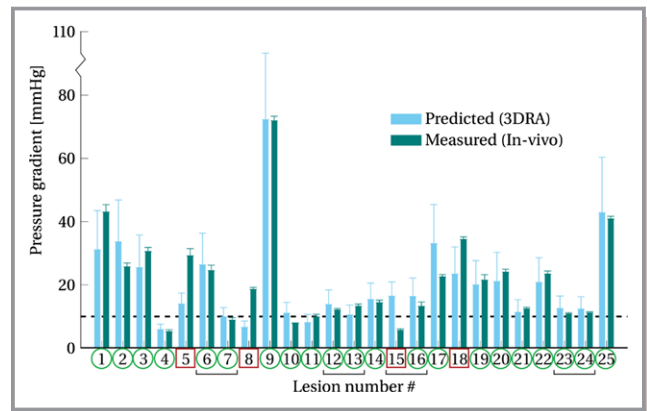


Figure 4. Calculated (blue) and in vivo measured (green) maximal pressure gradients observed after administering a vasodilator. The black markers below the lesion numbers indicate stenoses evaluated in the same patient but from different legs. A green circle around the lesion indicates overlap between the calculated and measured translesional pressure gradient. The red square indicates a nonoverlapping SD of the calculated and measured pressure gradient. The black dashed line indicates the cutoff for hemodynamic significant stenoses (≥ 10 mm Hg). 3DRA indicates 3-dimensional rotational angiography.

70%–100%), and a negative predictive value of 75% (95% CI, 53%–90%). The overall predictive value is 88% (95% CI, 68%–98%). On the basis of the in vivo measured hyperemic pressure gradients, 20 lesions were hemodynamic significant, of which 19 were treated. Although lesion 12 had a measured translesional pressure gradient of 12.1 ± 0.5 mm Hg, the interventionalist did not treat this lesion on the basis of visual assessment of the stenosis.

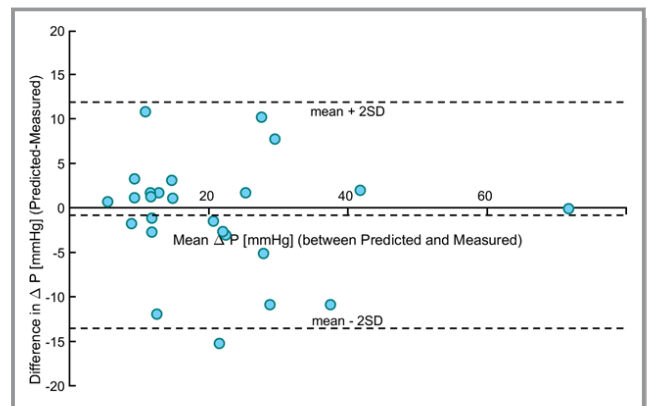


Figure 5. Bland-Altman plot demonstrating the bias (-0.9 mm Hg) between the calculated and measured translesional pressure gradient at maximal hyperemia. The 2 outer lines indicate the 2 SDs lower and higher than the mean bias (± 12.7 mm Hg).

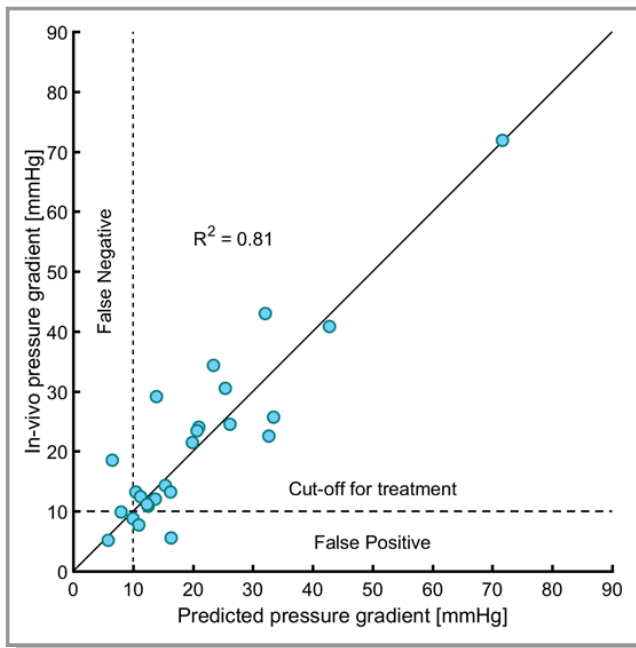


Figure 6. Correlation between in vivo measured and calculated pressure gradients. The black dashed lines indicate the cutoff for hemodynamic significant lesions (>10 mm Hg). The R^2 with respect to the line $y=x$ is 0.81.

Discussion

The aim of this study was to examine the feasibility of a computational model to predict the translesional pressure gradient across iliac artery stenosis under hyperemic conditions in an individual patient. The patient-specific geometry was obtained from 3DRA. During the same procedure, in vivo pressure measurements were performed to validate the predicted hyperemic pressure gradients, hereby avoiding possible bias introduced by disease progression. An empirical relation was derived to estimate the hyperemic flow lesion specifically. Study results show that the model is capable of calculating the hyperemic translesional pressure gradient over equivocal iliac artery stenosis patient specifically, by using 3DRA geometric input and the estimated hyperemic flow. Of

Table 2. Number of Significant Stenoses as Predicted by the Patient-Specific Computer Model With the Measured Intra-Arterial Hyperemic Pressure Gradient as a Reference

Predicted Pressure Gradient, mm Hg	Measured Pressure Gradient, mm Hg		
	<10	≥10	Total
<10	3	1	4
≥10	2	19	21
Total	5	20	25

A hemodynamic significant stenosis was defined as a pressure gradient of ≥10 mm Hg.

25 lesions, 21 showed good agreement (overlapping error bars) between the measured and calculated translesional pressure gradient. The model can distinguish between hemodynamic significant and nonsignificant lesions with 88% accuracy. In contrast, traditional modalities, such as peak systolic velocity ratios (measured by duplex ultrasonography) or geometry-based diagnosis (on the basis of visual inspection of digital subtraction angiography) had, compared with intra-arterial pressure measurements, a diagnostic accuracy of 77% to 81%^{19,20} and 71% to 81%,^{20,21} respectively. The feasibility of the computational model was assessed for patients with isolated iliac artery stenosis and for patients with iliac artery stenosis who also had downstream lesions.

Advantages of 3DRA-Based Predicted Translesional Pressure Gradient

The computer model provides the interventionalist with a good approximation of the patient-specific estimate of the pressure gradient within minutes, using the already available vascular geometry and empirically estimated hyperemic flow. The estimate of the pressure gradient can be obtained without performing any other measurements. Current results indicate that the computational model might be an aid to diagnose hemodynamic significant equivocal iliac artery stenosis during revascularization procedures, especially because only a few experts currently measure the hyperemic transstenotic pressure gradient in vivo.³ One could argue that, after acquiring access with a sheath in the common femoral artery, it is easy to advance an FFC to the aorta and measure the pressure gradient proximally and distally of the lesion simultaneously under hyperemic conditions. However, placing a 4F or 5F catheter across a stenosis causes a significant overestimation of the pressure gradient.²² Therefore, measuring pressure gradients using an FFC is a major pitfall and considered unreliable. Using the model, invasive pressure measurements can be left out, saving time and the necessity of using vasoactive drugs. When in doubt, one could just treat the iliac stenosis because of the excellent technical and clinical results⁵ and the low complication rates.²³ Using the model in the decision-making process could increase assessment accuracy and, thereby, prevent unnecessary treatment, resulting in fewer balloons and stents being used and reducing costs.

Disadvantages of 3DRA-Based Predicted Translesional Pressure Gradient

A disadvantage of our approach is that the patient-specific geometry assessment still requires a catheterization at the angi suite. As a consequence, patients who do not appear to

have a significant stenosis on the basis of visual assessment of the angiography are still exposed to iodinated contrast and radiation; valuable time of the patient and operators is spent in the angiosuite. This stresses the need for a model based on noninvasive preprocedural geometrical information (eg, contrast-enhanced magnetic resonance angiography or computed tomographic angiography). The method is available, but the accuracy and applicability need to be determined before the model can be used in the diagnosis of equivocal iliac artery stenosis on the basis of preprocedural modalities alone.

Another disadvantage is that axisymmetry was assumed, which neglects out-of-plane curvature. Therefore, the results presented are only validated for ordinary stenosis geometries and are unable to incorporate complex 3D geometries with flow patterns in 3 spatial directions (eg, vessel wall dissections [lesions 5 and 11]). Neglecting out-of-plane curvature might result in an underestimation of the calculated pressure gradient when compared with the actual pressure gradient. Moreover, because of the axisymmetry, no bifurcations can be incorporated and the pressure gradient can only be evaluated across a single-vessel segment.

The ability to simulate a complete vascular tree would allow us to investigate the relative contribution of multiple serial stenoses and virtually be able to evaluate different treatment strategies. For example, for a patient with multi-level disease, the outcome of treatment of the most proximal lesion, treatment of the most distal lesion, or even treatment of all identified lesions would allow us to select the treatment most beneficial to the patient. To incorporate multiple stenoses or bifurcations, 3D models are needed. Unfortunately, 3D models are computationally expensive and take days to be evaluated. A more time-efficient approach could be used through coupling the proposed approach with a fast 1-dimensional pulse-wave propagation model.²⁴ The combination of a 1-dimensional model and our approach can simulate pressure and flow waveforms through a complete vascular network in real time while describing the complex hemodynamic behavior across stenoses.

Future Improvements

A first improvement is an improvement of the empirical relation of the hyperemic flow estimate. The rationale for this approach is based on the work of Kaufman et al and de Jong et al.^{14,15} Kaufman et al found that the degree of vasodilator-enhanced flow higher than baseline diminishes linearly with increasing stenosis severity,¹⁵ whereas de Jong et al reported a linear relation between the minimal area at the neck of superficial femoral artery stenoses and the maximal mean hyperemic flow in dogs.¹⁴ By using such a linear relation, we assumed the resistance at the neck of the stenosis to be the flow-limiting resistance. Hence, it is recognized that the

calculation of the predicted pressure gradient might be unreliable in patients with a diseased microcirculatory system (eg, patients experiencing diabetes mellitus), because in those patients the peripheral resistance might become the flow-limiting resistance. The quality of this relation and its applicability might further improve if we include more patients in future studies (Data S1, Figure S1).

A second improvement for calculating the pressure gradient can be made by improving the quality of angiographic data in case of either obese patients (lesion 10) or patients having severe wall calcifications (lesion 15). The accuracy of the computational model might be influenced by the low-quality input data in these cases. Magnetic resonance angiograms or dual-energy

computed tomographic angiograms are less affected by arterial wall calcifications and are, therefore, considered good alternatives to be used in future studies. A third improvement might be to include collateral vessels that bypass the stenosis into the model. Because collateral vessels contribute to the distal perfusion pressure, their presence might result in overestimation of the predicted pressure gradient. However, it is expected that this will only occur in a few patients with equivocal stenosis because collateral vessels are mostly observed across severe stenosis (>80% lumen area reduction).^{25,26}

Finally, the total number of lesions evaluated in this study is limited. Although patients were selected on the basis of equivocal stenoses (duplex ultrasonography, 50%–75% diameter reduction), the number of lesions with a hyperemic translesional time-averaged pressure gradient between 5 and 15 mm Hg was limited (N=12). These lesions cause most doubt about the need for revascularization and are, therefore, of greatest clinical interest.

To investigate the true diagnostic value of the proposed approach, a second study has been initiated (DETECT-PAD study II, Dutch Trial Registry NTR6476) that aims to enlarge the study cohort by including another 50 patients. In addition, the ability of magnetic resonance angiography (N=25) and computed tomographic angiography (N=25) to replace 3DRA will be explored on their feasibility to be used as a basis for the pressure gradient calculations. Enrollment for participants in this second study is open.

Conclusion

This is the first study performed on iliac artery stenoses, evaluating the prediction of predicted translesional pressure gradient. We tested the feasibility of a patient-specific computational model and showed that the predicted translesional pressure gradient had good agreement with the in vivo measured pressure gradient (84%). Hemodynamic significant iliac artery stenosis ($\Delta p \geq 10$ mm Hg) can be identified with

88% accuracy. The model will be adapted to the applicability of a preprocedural imaging modality and will be optimized with more patients in future studies.

Acknowledgments

We sincerely thank the St Antonius Research fund, Volcano Inc, and the Dutch Endovascular Alliance.

Sources of Funding

The authors received unrestricted research grants from the St Antonius Research fund, Volcano Inc, and the Dutch Endovascular Alliance.

Disclosures

None.

References

- O'Donnell ME, Reid JA, Lau LL, Hannon RJ, Lee B. Optimal management of peripheral arterial disease for the non-specialist. *Ulster Med J*. 2011;80:33–41.
- Fish JH, Klein-Weigel P, Fraedrich G. Overview of the role of duplex ultrasound for treatment and surveillance of peripheral arterial disease. *J Patient Cent Res Rev*. 2015;2:104–111.
- de Boer SW, Heinen SGH, van den Heuvel DAF, van de Vosse FN, de Vries JPPM. How to define the hemodynamic significance of an equivocal iliofemoral artery stenosis: review of literature and outcomes of an international questionnaire. *Vascular*. 2017;1:1708538117700751. [Epub ahead of print]
- Hirsch AT, Haskal ZJ, Hertzler NR, Bakal CW, Creager MA, Halperin JL, Hiratzka LF, Murphy WRC, Olin JW, Puschett JB, Rosenfield KA, Sacks D, Stanley JC, Taylor LM, White CJ, White J, White RA. ACC/AHA 2005 practice guidelines for the management of patients with peripheral arterial disease (lower extremity, renal, mesenteric, and abdominal aortic). *Circulation*. 2006;113:e463–e654.
- Norgren L, Hiatt WR, Dormandy JA, Nehler MR, Harris KA, Fowkes FGR, Rutherford RB; TASC II Working Group. Inter-society consensus for the management of peripheral arterial disease. *Int Angiol*. 2007;26:81–157.
- Rajebi MR, Benenati MJ, Scherthaner MB, Walker G, Gandhi RT, Pena CS, Katzen BT. Reliability and accuracy of simple visual estimation in assessment of peripheral arterial stenosis. *J Vasc Interv Radiol*. 2015;26:890–896.
- Reiber JH, Serruys PW. Quantitative coronary angiography. In: Marcus M, Schelbert H, Skorton DJ, Wolf GL, eds. *Cardiac Imaging: A Companion to Braunwald's Heart Disease*. Philadelphia, Pennsylvania, USA: Saunders; 1991:211–280.
- Klein WM, van der Graaf Y, Seegers J, Spithoven JH, Buskens E, van Baal JG, Buth J, Moll FL, Overtoom TTC, van Sambeek MRHM, Mali WPTM. Dutch iliac stent trial: long-term results in patients randomized for primary or selective stent placement. *Radiology*. 2006;238:734–744.
- Bosch JL, Tetteroo E, Mali WP, Hunink MG; DUTCH ILIAC STENT TRIAL STUDY GROUP. Iliac arterial occlusive disease: cost-effectiveness analysis of stent placement versus percutaneous transluminalangioplasty. *Radiology*. 1998;208:641–648.
- Bosch JL, Haaring C, Meyerovitz MF, Cullen KA, Hunink MG. Cost-effectiveness of percutaneous treatment of iliac artery occlusive disease in the United States. *AJR Am J Roentgenol*. 2000;175:517–521.
- Morris PD, Ryan D, Morton AC, Lycett R, Lawford PV, Hose DR, Gunn JP. Virtual fractional flow reserve from coronary angiography: modeling the significance of coronary lesions: results from the VIRTU-1 (VIRTUal Fractional Flow Reserve From Coronary Angiography) study. *JACC Cardiovasc Interv*. 2013;6:149–157.
- Nakazato R, Park HB, Berman DS, Gransar H, Koo BK, Erglis A, Lin FY, Dunning AM, Budoff MJ, Malpeso J, Leipsic J, Min JK. Noninvasive fractional flow reserve derived from computed tomography angiography for coronary lesions of intermediate stenosis severity: results from the DeFACTO study. *Circ Cardiovasc Imaging*. 2013;6:881–889.
- Taylor CA, Fonte TA, Min JK. Computational fluid dynamics applied to cardiac computed tomography for noninvasive quantification of fractional flow reserve: scientific basis. *J Am Coll Cardiol*. 2013;61:2233–2241.
- de Jong JP, Westerhof N, Elzinga G. How to quantify an arterial stenosis: a study on the femoral arteries of dog and man. *Cardiovasc Res*. 1986;20:134–144.
- Kaufman SL, Fara JW, Udoff EJ, Harrington DP, White R. Hemodynamic effects of vasodilators across iliac stenoses in dogs. *Invest Radiol*. 1979;14:471–475.
- Taylor KJ, Burns PN, Woodcock JP, Wells PN. Blood flow in deep abdominal and pelvic vessels: ultrasonic pulsed-Doppler analysis. *Radiology*. 1985;154:487–493.
- Hulsen M. *TFEM Users Guide*. Eindhoven, the Netherlands: Eindhoven University of Technology; 2008.
- Newcombe RG. Two-sided confidence intervals for the single proportion: comparison of seven methods. *Stat Med*. 1998;17:857–872.
- Heinen SGH, de Boer SW, van den Heuvel DAF, Huberts W, Dekker P, van de Vosse FN, Delhaas T, de Vries JPPM. Hemodynamic significance assessment of equivocal iliac artery stenoses by comparing duplex ultrasonography with intra-arterial pressure measurements. *J Cardiovasc Surg (Torino)*. 2017 <https://www.minervamedica.it/en/journals/cardiovascular-surgery/article.php?cod=R37Y2018N01A0037>. Accessed November 18, 2017. [Epub ahead of print]
- Legemate DA, Teeuwen C, Hoeneveld H, Eikelboom BC. Value of duplex scanning compared with angiography and pressure measurement in the assessment of aortoiliac arterial lesions. *Br J Surg*. 1991;78:1003–1008.
- Breslau PJ, Jörning PJ, Greep JM. Assessment of aortoiliac disease using hemodynamic measures. *Arch Surg*. 1985;120:1050–1052.
- Garcia LA, Carrozza JP. Physiologic evaluation of translesion pressure gradients in peripheral arteries: comparison of pressure wire and catheter-derived measurements. *J Interv Cardiol*. 2007;20:63–65.
- Rholl K, van Breda A. Percutaneous intervention for aortoiliac disease. In: Strandness DE, van Breda A, eds. *Vascular diseases: surgical & interventional therapy*. New York, NY: Churchill Livingstone; 1994:433–466.
- Kroon W, Huberts W, Bosboom M, van de Vosse FN. A numerical method of reduced complexity for simulation vascular hemodynamics using coupled 0D lumped and 1D wave propagation models. *Comput Math Methods Med*. 2012;2012:156094.
- Cohen M, Sherman W, Rentrop KP, Gorlin R. Determinants of collateral filling observed during sudden controlled coronary artery occlusion in human subjects. *J Am Coll Cardiol*. 1989;13:297–303.
- Pohl T, Seiler C, Billinger M, Herren E, Wustmann K, Mehta H, Windecker S, Eberli FR, Meier B. Frequency distribution of collateral flow and factors influencing collateral channel development: functional collateral channel measurement in 450 patients with coronary artery disease. *J Am Coll Cardiol*. 2001;38:1872–1878.

SUPPLEMENTAL MATERIAL

Data S1

Although the true correlation is unknown, it can be shown that with increasing number of lesions the correlation will become more accurate and with sufficient number of lesions finally will approach the true population averaged correlation. First, the hyperemic flow was estimated from the patient-specific geometry and the measured hyperemic pressure gradient using an inverse modeling approach. The estimated hyperemic flows were correlated to the area at the neck of the stenoses (A_s) using the leave-one-out method. Applying the leave-one-out method for every possible subset of lesions will result in a different correlation. The mean and standard deviation (SD) of all possible subsets for a given number of lesions were determined. Convergence towards the populations averaged correlation for increasing number of lesions is shown for the intersect with the y-axis (Figure 6A) and the angle of the line with the x-axis (Figure 6B). For this convergence analysis all lesions were used except for the lesion that was identified as outlier given a total of $N = 24$ lesions (Figure S1C).

From Figure S1A & S1B, it can be observed that the estimates for the angle and intersect indeed become more accurate with increasing number of patients. The study averaged correlation of the current cohort ($N = 24$) resulted in an angle and intersect of 51.6° and 8.6 mL/s respectively. With increasing number of lesions the correlation will become more accurate.

Data S2

The linear correlation between the back engineered hyperemic flow (q_{hyp}) and the area at the neck of the stenosis (A_s) is given by the least squares fit through the data resulting in

$$q_{hyp} = aA_s + q_0. \quad \text{Eq.1}$$

with a the slope and q_0 the intersect with the y-axis indicating the remaining (collateral) hyperemic flow given that the artery is occluded ($A_s = 0$). The uncertainties in the estimated slope (a) and intercept (q_0), assumed that all points have equal error, are:

$$a_{err} = S \cdot \sqrt{\frac{n}{(n \sum A_s^2) - (\sum A_s)^2}}, \quad \text{Eq. 2}$$

$$q_{0_err} = S \cdot \sqrt{\frac{\sum A_s^2}{(n \sum A_s^2) - (\sum A_s)^2}}, \quad \text{Eq. 3}$$

respectively with S

$$S = \sqrt{\frac{\sum (q_{hyp} - aA_s - q_0)^2}{n-2}}. \quad \text{Eq. 4}$$

By removing the identified outlier and applying the leave-one-out method, $n = 23$. It was assumed that all points have an equal error.

Figure S1. Convergence of the hyperemic flow towards the population averaged correlation as function of the number of included lesions. **(A)** shows the convergence of the flow (q_0) at $x = 0$. **(B)** shows the angle of the correlation line with the x-axis. It can be observed that the estimation of q_0 and the angle become more accurate with increasing number. **(C)** shows the correlation for the total study cohort.

